An asymptotic-preserving scheme for linear kinetic equation with fractional diffusion limit

Li Wang* Bokai Yan †

November 11, 2015

Abstract

We present a new asymptotic-preserving scheme for the linear Boltzmann equation which, under appropriate scaling, leads to a fractional diffusion limit. Our scheme rests on novel micro-macro decomposition to the distribution function, which splits the original kinetic equation following a *reshuffled* Hilbert expansion. As opposed to classical diffusion limit, a major difficulty comes from the *fat tail* in the equilibrium which makes the truncation in velocity space depending on the small parameter. Our idea is, while solving the macro-micro part in a truncated velocity domain (truncation only depends on numerical accuracy), to incorporate an integrated tail over the velocity space that is beyond the truncation, and its major component can be precomputed once with any accuracy. Such an addition is essential to drive the solution to the correct asymptotic limit. Numerical experiments validate its efficiency in both kinetic and fractional diffusive regimes.

Keywords: fractional diffusion, heavy tail, asymptotic-preserving scheme, micro-macro decomposition

1 Introduction

The linear Boltzmann equation describes the time evolution of particle distribution that undergoes a free transport and collision with the background. The distribution function $f(t,x,v)$ depending on time $t>0$, position $x\in\mathbf{R}^N$ and velocity $v\in\mathbf{R}^N$ solves:

$$\partial_t f + v\cdot\nabla_x f = \mathcal{L}(f), \qquad (t,x,v)\in(0,\infty)\times\mathbf{R}^N\times\mathbf{R}^N, \tag{1.1}$$

$$f(0,x,v) = f_0(x,v), \tag{1.2}$$

where the collision $\mathcal{L}$ takes the form

$$\mathcal{L}(f) = \int_{\mathbf{R}^N}\left[\sigma(x,v,v')f(t,x,v') - \sigma(x,v',v)f(t,x,v)\right]\,\mathrm{d}v'.$$

Here $\sigma(x,v,v')\geq 0$ is the transition probability, which, under some classical conditions [9, 16] gives rise to a unique equilibrium function $\mathcal{F}(v)\geq 0$ satisfying

$$\mathcal{L}(\mathcal{F}) = 0, \qquad \mathcal{F}(v) = \mathcal{F}(-v), \qquad \int_{\mathbf{R}^N}\mathcal{F}(v)\,\mathrm{d}v = 1 \quad \text{for all} \quad x\in\mathbf{R}^N. \tag{1.3}$$

*Department of Mathematics, University of California, Los Angeles, 520 Portola Plaza, Los Angeles, CA 90095 (liwang@math.ucla.edu).

†Department of Mathematics, University of California, Los Angeles, 520 Portola Plaza, Los Angeles, CA 90095 (byan@math.ucla.edu)

Let ϵ be the ratio of mean free path over the macroscopic length scale, we rescale the space variable $\tilde{x} = \frac{x}{\epsilon}$ and time variable $\tilde{t} = \frac{t}{\theta(\epsilon)}$, where $\theta(\epsilon)$ that satisfies $\lim_{\epsilon \to 0} \theta(\epsilon) = 0$ will be specified later. Then equation (1.1) in the dimensionless form, upon suppression of tildes, reads

$$\theta(\epsilon)\partial_t f + \epsilon v \cdot \nabla_x f = \mathcal{L}(f). \tag{1.4}$$

Typically when the mean free path is small and time scale is large, i.e., $\theta(\epsilon) = \epsilon^2$, the distribution of the particles is assumed to be at equilibrium given by a Maxwellian distribution function, and density evolution solves a diffusion equation

$$\partial_t \rho - \nabla_x (D \nabla_x \rho) = 0,$$

where D is a diffusion matrix

$$D = \int_{R^n} v \otimes \mathcal{L}^{-1}(v\mathcal{F})\, \mathrm{d}v.$$

For an extensive review of these studies, the reader is referred to [2, 3, 9, 14]. However, if the equilibrium is not a Maxwellian but rather a heavy tail function, i.e.,

$$\mathcal{F}(v) \sim \frac{\kappa_0}{|v|^{N+\alpha}}, \qquad 1 < \alpha < 2, \qquad \text{as } |v| \to \infty,$$

the classical diffusion theory fails because the diffusion matrix D is infinite. Instead, we should consider a different time scale $\theta(\epsilon) = \epsilon^\alpha$, in which case the limit behavior is governed by a fractional (anomalous) diffusion equation. Such an equilibrium arises in numerous areas of applications such as granular plasmas with dissipative collision [5, 4], astrophysical plasmas [18] and economy [10]. A rigorous derivation is undertaken in [17] via the Fourier-Laplace transform and extended in [16] for a more general space dependent or anisotropic scattering based on a weak formulation and particular choice of test function. It is revisited in a more recent work [1] following a Hilbert expansion approach which is capable in proving strong convergence results.

As opposed to sound analytical investigations, numerically solving the equation with scaling (1.4) is still at its infancy. Our goal in this paper is to provide a numerical scheme for the linear Boltzmann equation (1.4) efficient in both kinetic ($\epsilon \sim O(1)$) and anomalous diffusive ($\epsilon \ll 1$) regimes. More precisely, we want a scheme designed for the kinetic equation (1.4) preserves the asymptotic limit at the discrete level such that it automatically becomes a macroscopic solver for the fractional diffusion equation (2.4) (2.17) as $\epsilon \to 0$. This is the so called asymptotic-preserving (AP) schemes put forth by Jin [12]. A natural thought is to use implicit treatments on stiff terms, but this is impractical due to the non locality of the collision operator and the presence of the stiff convection. As such a difficulty has already appeared in the classical diffusive scaling, one might refer to some kinds of decompositions such as even-odd decomposition [13] or macro-micro decomposition [15, 6, 7] to separate the non-stiff part from the stiff part. However, since our limit is obtained through a *reshuffled* Hilbert expansion (the gain term in the collision switches with the convection term), previous methods do not apply. Here we propose a variant decomposition for the distribution f which splits equation (1.4) in a way that bares analogy with the reshuffled Hilbert expansion. Besides stiffness, another major difficulty lies in the fat tail which renders any truncation in velocity space inaccurate since the tail plays a significant role for small ϵ. Our idea consists of adding a tail to the decomposition, and evaluate its average value over the whole velocity space, whose major component can be precomputed once with any accuracy. We would like to point out a related work by Crouseilles-Hivert-Lemou [8] in which they consider the same problem but using a very different approach.

The rest of the paper is organized as follows. In the next section we give a brief review on the basic scaling of (1.4) and how it leads to the fractional limit. Section 3 is devoted to the major part of our scheme when the scattering is space inhomogeneous. The key ideas include: a system decomposition, a velocity truncation, and a tail compensation. In Section 4, we extend the scheme to a space inhomogeneous scattering with a simplification based on the idea of changing of space variable. Numerical examples are given in Section 5 to illustrate the efficiency, accuracy and AP properties of the new scheme. Finally the paper is concluded in Section 6.

2 Scaling and fractional diffusion limit

In this section, we specify the assumptions on the transition probability and review in brief the fractional diffusion limit of (1.4) under the appropriate choice of time scale $\theta(\epsilon)$. The rigorous theory has been carried out in [1, 16, 17] using various approaches such as the Laplace-Fourier transform, moment method and Hilbert expansion. We only pick up the latter approach as it facilitates our numerical scheme.

Rewrite the collision into a more convenient form

$$\mathcal{L}(f) \;=\; \int_{\mathbf{R}^N} \phi(x,v,v')\left[\mathcal{F}(v)f(t,x,v') - \mathcal{F}(v')f(t,x,v)\right]\,\mathrm{d}v' := K(f)\mathcal{F} - \nu(x,v)f,$$

where $\phi(x,v,v')$ is the scattering cross-section satisfying $\phi(x,v,v') = \phi(x,v',v)$. Then the gain term $K(f)\mathcal{F}$ and the loss term $\nu(x,v)f$ are defined as

$$K(f)\mathcal{F} = \int_{\mathbf{R}^N} \phi(x,v,v')f(t,x,v')\,\mathrm{d}v'\mathcal{F}, \qquad \nu(x,v)\mathcal{F} = \int_{\mathbf{R}^N} \phi(x,v',v)\mathcal{F}(v')\,\mathrm{d}v'\mathcal{F}, \tag{2.1}$$

where $\nu(x,v)$ is the collision frequency. Now we make the following assumptions.

(A1) The cross-section $\phi \geq 0$ is locally integrable on $\mathbf{R}^{2N}$, and the collision frequency is locally integrable on $\mathbf{R}^N$ and satisfies $\nu(x,-v) = \nu(x,v) > 0$ for all $v \in \mathbf{R}^N$.

(A2) The equilibrium $\mathcal{F}$ is assumed to be independent of x and has a heavy tail in v, satisfying

$$\mathcal{F}(v) = \begin{cases} \frac{\kappa_0}{|v|^{N+\alpha}} & \text{for } |v| \geq 1 \\ \kappa_0 & \text{for } 0 \leq |v| < 1 \end{cases} \tag{2.2}$$

for some $\alpha \in (1,2)$ and κ_0 is chosen such that $\mathcal{F}$ integrates to 1 as in (1.3).

In this paper we use the notation $\langle\cdot\rangle = \int \cdot\,\mathrm{d}v$.

We first consider the simplest case (isotropic) when $\phi(v,v') = 1$, $\mathcal{L}$ rewrites

$$\mathcal{L}(f) = \int_{\mathbf{R}^N} f(v')\,\mathrm{d}v'\mathcal{F}(v) - f(v) = \langle f\rangle\,\mathcal{F} - f(v), \tag{2.3}$$

and thus $\ker(\mathcal{L}) = \left\{\rho(x,t)\mathcal{F}(v);\ \rho : \mathbf{R}^N \times \mathbf{R} \to \mathbf{R}\right\}$. The following result concerns the fractional diffusion limit.

Theorem 1. *[1] Let f be the solution of (1.4) with $\theta(\epsilon) = \epsilon^\alpha$, $\mathcal{L}(f)$ given by (2.3) with assumption (A1)–(A2) and initial condition $f_{in}(x,v) = \rho_{in}(x)\mathcal{F}(v)$ such that $\rho_{in} \in H^3(\mathbf{R}^N)$. Then*

$$\| f - \rho_0\mathcal{F} \|_{L^\infty(0,\infty;L^2_{\mathcal{F}^{-1}}(\mathbf{R}^N\times\mathbf{R}^N))} \to 0 \qquad \text{as } \epsilon \to 0,$$

where ρ_0 solves

$$\begin{cases} \partial_t \rho_0 + \kappa(-\triangle)^{\frac{\alpha}{2}} \rho_0 = 0, \\ \rho_0(x,0) = \rho_{in}(x), \end{cases} \tag{2.4}$$

with

$$\kappa = \kappa_0 \int_{\mathbf{R}^N} \frac{(w\cdot e)^2}{1+(w\cdot e)^2} \frac{1}{|w|^{N+\alpha}}\,\mathrm{d}w. \tag{2.5}$$

Here the norm $L^2_{\mathcal{F}^{-1}}$ is defined as $\| f(t,x,v) \|^2_{L^2_{\mathcal{F}^{-1}(\mathbf{R}^N\times\mathbf{R}^N)}} = \int_{\mathbf{R}^N}\int_{\mathbf{R}^N} f^2 \mathcal{F}^{-1}\,\mathrm{d}v\,\mathrm{d}x$.

To proceed with the derivation of the limit in the above theorem, we need the following lemma first.

Lemma 2. *Sending $\epsilon \to 0$, we have*

$$\frac{1}{\epsilon^\alpha}\int_{\mathbf{R}^N} \frac{i\epsilon v\cdot k}{1+i\epsilon v\cdot k}\mathcal{F}(v)\,\mathrm{d}v \to \kappa|k|^\alpha \tag{2.6}$$

with κ given in (2.5).

Proof. Break the integral into two parts

$$\begin{aligned} & \frac{1}{\epsilon^\alpha}\int_{\mathbf{R}^N} \frac{i\epsilon v\cdot k}{1+i\epsilon v\cdot k}\mathcal{F}(v)\,\mathrm{d}v \\ = \;& \frac{1}{\epsilon^\alpha}\int_{|v|\le 1} \frac{(\epsilon v\cdot k)^2}{1+(\epsilon v\cdot k)^2}\mathcal{F}(v)\,\mathrm{d}v + \frac{1}{\epsilon^\alpha}\int_{|v|>1} \frac{(\epsilon v\cdot k)^2}{1+(\epsilon v\cdot k)^2}\frac{\kappa_0}{|v|^{N+\alpha}}\,\mathrm{d}v \\ := \;& I_1 + I_2, \end{aligned} \tag{2.7}$$

where

$$I_1 \le \kappa_0 \epsilon^{2-\alpha}\int_{|v|\le 1}(v\cdot k)^2\,\mathrm{d}v \to 0 \qquad \text{as } \epsilon\to 0. \tag{2.8}$$

Denote $\omega = \epsilon v|k|$, then

$$\begin{aligned} I_2 - \kappa|k|^\alpha\hat{\rho}_0 &= |k|^\alpha \int_{|\omega|\le\epsilon|k|} \frac{(\omega\cdot e)^2}{1+(\omega\cdot e)^2}\frac{\kappa_0}{|\omega|^{N+\alpha}}\,\mathrm{d}\omega \\ &\le |k|^\alpha \int_{S^{N-1}}\int_{|\omega|\le\epsilon|k|} \kappa_0|\omega|^{1-\alpha}\,\mathrm{d}|\omega| dS^{N-1} \to 0 \end{aligned} \tag{2.9}$$

as $\epsilon\to 0$. □

Now consider the Hilbert expansion of f,

$$f = f_0 + g_1 + g_2 + \cdots,$$

where the leading terms solve

$$0 = \mathcal{L}(f_0) = \langle f_0\rangle\,\mathcal{F} - f_0, \tag{2.10}$$

$$\epsilon v\cdot\nabla_x(f_0+g_1) = -g_1, \tag{2.11}$$

$$\epsilon^\alpha \partial_t f_0 = \langle g_1\rangle\,\mathcal{F} + \mathcal{L}(g_2). \tag{2.12}$$

As written, (2.11) (2.12) differ from classical diffusion limit in that the terms $\langle g_1 \rangle$ and $\epsilon v \cdot \nabla_x g_1$ are reshuffled under the observation that the advection term and the loss part of the collision operator are of the same order whereas the gain term is of higher order [1]. Then (2.10) yields

$$f_0 = \rho_0 \mathcal{F}(v), \tag{2.13}$$

and the solvability condition enables us to write (2.12) into

$$\epsilon^\alpha \partial_t \rho_0 = \langle g_1 \rangle . \tag{2.14}$$

To solve for g_1 from (2.11), we take the Fourier transform with respect to x. Denote $\hat{g}(t,k,v)$ the Fourier transform of $g(t,x,v)$, then we have

$$(1 + i\epsilon v \cdot k)\hat{g_1} = -i\epsilon v \cdot k \hat{f}_0,$$

and thus

$$\frac{1}{\epsilon^\alpha} \langle \hat{g_1} \rangle \quad = \quad -\frac{1}{\epsilon^\alpha} \int_{\mathbf{R}^N} \frac{i\epsilon v \cdot k}{1 + i\epsilon v \cdot k} \mathcal{F}(v) \, \mathrm{d}v \hat{\rho}_0, \tag{2.15}$$

which leads to $\frac{1}{\epsilon^\alpha} \langle \hat{g_1} \rangle \to \kappa |k|^\alpha \hat{\rho}_0$ as $\epsilon \to 0$ thanks to Lemma 2. Plug the limit of (2.15) into (2.14) results in (2.4).

For a more general case when the collision cross section σ depends on x, we assume further that the collision frequency is regular enough and has a nice asymptotic behavior for large v, i.e.,

(A3) $\partial_x^m \nu \in L^\infty(\mathbf{R}^N \times \mathbf{R}^N)$ for all multi-indice m such that $|m| \le 4$,
$\nu(x,v) = \nu_0(x)$ for $|v| > 1$ (2.16)

we have the following result for space inhomogeneous collision.

Theorem 3. *[1] Assume $\mathcal{F}$, ν satisfy (A1), (A2) and (2.16). Let f be the solution of (1.4) with $\theta(\epsilon) = \epsilon^\alpha$ and initial condition $f_{in}(x,v) = \langle f_{in} \rangle (x) \mathcal{F}(v) = \rho_{in}(x) \mathcal{F}(v)$ satisfies $\rho_{in}(x) \in H^4(\mathbf{R}^n)$, then*

$$\| f - \rho_0 F \|_{L^\infty(0,\infty;L^2_{\mathcal{F}^{-1}}(\mathbf{R}^N \times \mathbf{R}^N))} \to 0, \qquad \text{as } \epsilon \to 0,$$

where ρ_0 solves

$$\begin{cases} \partial_t \rho_0 + L(\rho_0) = 0, \\ \rho_0(x,0) = \rho_{in}(x), \end{cases} \tag{2.17}$$

where L is an elliptic operator defined by the singular integral

$$L(\rho) = \kappa_0 P.V. \int_{\mathbf{R}^N} \gamma(x,y) \frac{\rho(x) - \rho(y)}{|y-x|^{N+\alpha}} \, \mathrm{d}y \tag{2.18}$$

with

$$\gamma(x,y) = \nu_0(x)\nu_0(y) \int_0^\infty z^\alpha e^{-z \int_0^1 \nu_0((1-s)x + sy) ds} \, \mathrm{d}z. \tag{2.19}$$

This theorem can be proved in a similar manner as the previous case except that one can not use the Fourier transform because of the convolution that results from a space dependent collision. Instead, one seeks an integral formulation for the inverse operator of $\nu(x) + \epsilon v \cdot \nabla_x$.

Remark 4. In the case when $\phi(x,v,v') = 1$, $\nu(v) \equiv 1$ and thus $\nu_0 = 1$. Then (2.18) reduces to

$$L(\rho) = \kappa_0 P.V. \int_{\mathbf{R}^N} \frac{\rho(x) - \rho(y)}{|y-x|^{N+\alpha}} \, \mathrm{d}y, \tag{2.20}$$

which is the integral representation of $\kappa(-\triangle)^{\frac{\alpha}{2}}$ with κ defined in (2.5). Hence, we recover (2.4).

3 Numerical schemes for the space homogeneous cross section

As written, equation (1.4) contains two different scales, both of which render any explicit numerical scheme extremely expensive when ϵ is small. An implicit scheme is often expected, but it always results in a large algebraic system that is hard to invert. In this section, we consider equation (1.4) with collision (2.3), which, as simple as it looks, contains almost all the numerical difficulties that one may encounter as explained in the introduction. Our scheme includes two major components: a system decomposition and a velocity truncation with tail compensation. We will explain them in detail in the subsequent subsections.

3.1 System decomposition

When more than one scale appears in an equation, there is always a need to separate them. This section is devoted to splitting the original kinetic equation into two sub-equations that enables an implicit treatment of the stiff terms. When the collision takes the form of (2.3), the initial value problem reads

$$\begin{cases} \epsilon^\alpha \partial_t f + \epsilon v \cdot \nabla_x f = \langle f \rangle \mathcal{F} - f, \\ f(0,x) = f_{\text{in}}(x). \end{cases} \tag{3.1}$$

Decompose f into a macroscopic part and a microscopic part following the spirit of the Chapman-Enskog expansion:

$$f = \rho \mathcal{F} + g, \tag{3.2}$$

where $\rho\mathcal{F}$ accounts for the equilibrium part (in the limit $\epsilon \to 0$, ρ converges to the solution of the fractional diffusion equation) whereas g measures the non-equilibrium perturbation. Then it follows that

$$\epsilon^\alpha \partial_t(\rho\mathcal{F} + g) + \epsilon v \cdot \nabla_x(\rho\mathcal{F} + g) = \langle \rho\mathcal{F} + g \rangle \mathcal{F} - (\rho\mathcal{F} + g),$$

which can be split into two sub-equations as suggested by the Hilbert expansion (2.10)–(2.12):

$$\epsilon^\alpha \partial_t \rho = \langle g \rangle, \tag{3.3}$$

$$\epsilon^\alpha \partial_t g + \epsilon v \cdot \nabla_x(\rho\mathcal{F} + g) = -g, \tag{3.4}$$

where we have omitted $\mathcal{F}$ on both sides of (3.3). A major difference between this macro-micro decomposition and the one in [15] is that g has mass here, i.e., $\langle g \rangle \neq 0$ for finite ϵ. To get appropriate initial condition for both ρ and g, notice that in the limit $\epsilon \to 0$, we have $\epsilon v \cdot \nabla_x(\rho\mathcal{F} + g) = -g$ from (3.4), whose average implies $\epsilon \langle v \cdot \nabla_x f \rangle = -\langle g \rangle$, which suggests the following initial value decomposition

$$\begin{cases} \rho_{\text{in}} = \langle f_{\text{in}} \rangle - \langle g_{\text{in}} \rangle = \langle f_{\text{in}} + \epsilon v \cdot \nabla_x f_{\text{in}} \rangle, \\ g_{\text{in}} = f_{\text{in}} - \rho_{\text{in}} \mathcal{F}. \end{cases} \tag{3.5}$$

Then equations (3.3) (3.4) with initial condition (3.5) constitute an alternative formulation for (3.1), and serve as a building block for our numerical schemes. First we have the following propositions regarding the relationship between the solutions to these two systems.

Proposition 5. *If (ρ, g) solve (3.3)(3.4) with initial data (3.5), then $f = \rho\mathcal{F} + g$ is a solution to (3.1). Both systems have the property of energy dissipation $\frac{\mathrm{d}}{\mathrm{d}t} E_f \leq 0$, where the energy is defined by*

$$E_f = \left(\iint f^2 \mathcal{F}^{-1} \,\mathrm{d}x \,\mathrm{d}v \right)^{1/2} = \left(\iint (\rho\mathcal{F} + g)^2 \mathcal{F}^{-1} \,\mathrm{d}x \,\mathrm{d}v \right)^{1/2}. \tag{3.6}$$

Proof. It is easy to show that $f = \rho\mathcal{F} + g$ is a solution to (3.1) if (ρ, g) solve (3.3)(3.4) with initial data (3.5) by simply adding the equations, so we only prove the energy dissipation property. For the original system, multiply (3.1) by $2f\mathcal{F}^{-1}$ and integrate in both x and v, it becomes

$$\frac{\mathrm{d}}{\mathrm{d}t}\iint f^2\mathcal{F}^{-1}\,\mathrm{d}x\,\mathrm{d}v = \frac{2}{\epsilon^\alpha}\iint \left(\langle f\rangle\,\mathcal{F} - f\right) f\mathcal{F}^{-1}\,\mathrm{d}x\,\mathrm{d}v.$$

Notice that

$$\langle f\rangle^2 \le \int f^2\mathcal{F}^{-1}\,\mathrm{d}v \int \mathcal{F}\,\mathrm{d}v = \int f^2\mathcal{F}^{-1}\,\mathrm{d}v \tag{3.7}$$

by the Cauchy-Schwartz inequality, we have $\frac{\mathrm{d}}{\mathrm{d}t}\int f^2\mathcal{F}^{-1}\,\mathrm{d}x\,\mathrm{d}v \le 0$. Similarly for the splitted system (3.3) (3.4), multiply (3.3) by $\rho\mathcal{F}$ and (3.4) by $g\mathcal{F}^{-1}$ and integrate both of them in x and v, we have, by adding them together,

$$\begin{aligned}\iint \left[\epsilon^\alpha\partial_t\left(\frac{1}{2}\rho^2\mathcal{F} + \frac{1}{2}\frac{g^2}{\mathcal{F}} + \rho g\right) + \epsilon v\cdot\nabla_x(\rho\mathcal{F}+g)\frac{g}{\mathcal{F}}\right]\,\mathrm{d}x\,\mathrm{d}v &= \iint\left[\rho\mathcal{F}\,\langle g\rangle - \frac{g^2}{\mathcal{F}} + \epsilon^\alpha\partial_t(\rho g)\right]\,\mathrm{d}x\,\mathrm{d}v\\ = \iint\left[\rho\mathcal{F}\,\langle g\rangle - \frac{g^2}{\mathcal{F}} + \langle g\rangle\, g - \rho g - \epsilon\rho v\cdot\nabla_x(\rho\mathcal{F}+g)\right]\,\mathrm{d}x\,\mathrm{d}v.&\end{aligned} \tag{3.8}$$

Notice that $\iint \epsilon v\cdot\nabla_x g\frac{g}{\mathcal{F}}\,\mathrm{d}x\,\mathrm{d}v = \iint \epsilon\rho v\cdot\nabla_x\rho\mathcal{F}\,\mathrm{d}x\,\mathrm{d}v = 0$ and $\iint \rho\mathcal{F}\,\langle g\rangle\,\mathrm{d}x\,\mathrm{d}v = \iint \rho g\,\mathrm{d}x\,\mathrm{d}v$, (3.8) reduces to

$$\frac{\mathrm{d}}{\mathrm{d}t}\int\frac{\epsilon^\alpha}{2}\left\langle\frac{(\rho\mathcal{F}+g)^2}{\mathcal{F}}\right\rangle\,\mathrm{d}x + \int\langle\epsilon v g\cdot\nabla_x\rho\rangle\,\mathrm{d}x = \int\left[\langle g\rangle^2 - \left\langle\frac{g^2}{\mathcal{F}}\right\rangle - \epsilon\rho\,\langle v\cdot\nabla_x g\rangle\right]\,\mathrm{d}x,$$

which readily implies

$$\frac{\mathrm{d}}{\mathrm{d}t}\iint(\rho\mathcal{F}+g)^2\mathcal{F}^{-1}\,\mathrm{d}x\,\mathrm{d}v = \frac{2}{\epsilon^\alpha}\int\left[\langle g\rangle^2 - \left\langle\frac{g^2}{\mathcal{F}}\right\rangle\right]\,\mathrm{d}v.$$

Then by a similar inequality as (3.7), its right hand side is nonpositive. □

Armed with the above result, we can bound both ρ and g separately.

Proposition 6. *If (ρ, g) solve (3.3)(3.4) with initial data (3.5), then $\rho \in L^\infty(0,\infty;L^2(\mathbf{R}^N))$, $g \in L^\infty(0,\infty;L^2_{\mathcal{F}^{-1}}(\mathbf{R}^N\times\mathbf{R}^N))$, i.e.*

$$E_\rho := \left(\int\rho^2\,\mathrm{d}x\right)^{1/2} \qquad \text{and} \qquad E_g := \left(\iint\frac{g^2}{\mathcal{F}}\,\mathrm{d}x\,\mathrm{d}v\right)^{1/2} \tag{3.9}$$

are both uniformly bounded in time.

Proof. Multiplying ρ on both sides of (3.3) and integrating over x, one has

$$\begin{aligned}\frac{1}{2}\epsilon^\alpha\partial_t\int\rho^2\,\mathrm{d}x = \int\rho\,\langle g\rangle\,\mathrm{d}x &= \iint\rho(f-\rho\mathcal{F})\,\mathrm{d}v\,\mathrm{d}x\\ &= \iint\rho f\,\mathrm{d}v\,\mathrm{d}x - \int\rho^2\,\mathrm{d}x\\ &\le \left(\int\rho^2\,\mathrm{d}x\right)^{1/2}\left(\iint\frac{f^2}{\mathcal{F}}\,\mathrm{d}v\,\mathrm{d}x\right)^{1/2} - \int\rho^2\,\mathrm{d}x.\end{aligned}$$

With the definitions (3.6) and (3.9), this can be written as

$$\frac{1}{2}\epsilon^\alpha \partial_t E_\rho^2 \le E_\rho(E_f - E_\rho),$$

then

$$\epsilon^\alpha \partial_t E_\rho \le E_f - E_\rho. \tag{3.10}$$

Notice that E_f decays with time from Proposition 5, E_ρ is uniformly bounded in time. As for E_g, one has

$$E_g^2 = \iint (f - \rho\mathcal{F})^2 \mathcal{F}^{-1}\,\mathrm{d}v\,\mathrm{d}x \le 2\iint (f^2 + (\rho\mathcal{F})^2)\mathcal{F}^{-1}\,\mathrm{d}v\,\mathrm{d}x = 2(E_f^2 + E_\rho^2), \tag{3.11}$$

therefore E_g is also uniformly bounded in time. □

At this point, we would like emphasis that our decomposition (3.3) (3.4) is well-posed: the existence is guaranteed due to the linearity of the system and the stability directly follows Proposition 6.

3.2 First order semi-discretization in time

We now give a first order temporal semi-discrete scheme based on the splitting (3.3) (3.4),

$$\begin{cases} \epsilon^\alpha \dfrac{\rho^{n+1} - \rho^n}{\Delta t} = \left\langle g^{n+1} \right\rangle, \\ \epsilon^\alpha \dfrac{g^{n+1} - g^n}{\Delta t} + \epsilon v \cdot \nabla_x (\rho^* \mathcal{F} + g^{n+1}) = -g^{n+1}, \end{cases} \tag{3.12}$$

where the initial data is given by (3.5). Here ρ^* can be either ρ^{n+1} or ρ^n, and the resulting limit scheme will be implicit or explicit for the fractional diffusion equation.

Given ρ^n and g^n, the numerical approximations at time t^n, one first solves for g^{n+1} from the second equation. Then plug it into the first equation to obtain ρ^{n+1}. Note that solving for g^{n+1} involves the inversion of an unsymmetrical matrix from the discretization of the first order derivative $v \cdot \nabla_x$. For simplicity we assume periodic boundary condition in this paper, and solve for g^{n+1} by the spectral method. More specifically, we take the Fourier transform of both equations in (3.12) and evolve $\hat{\rho}$ and $\hat{g}$ in the Fourier space. ρ and g is obtained by inverse Fourier transform at the final time.

One can formally check the AP property. Taking the Fourier transform (in x direction) of the second equation in (3.12) gives

$$\epsilon^\alpha \frac{\hat{g}^{n+1} - \hat{g}^n}{\Delta t} + i\epsilon v \cdot k(\hat{\rho}^* \mathcal{F} + \hat{g}^{n+1}) = -\hat{g}^{n+1}.$$

Upon neglecting the high order term ϵ^α (we verify this point in Section 5.2 numerically), one has

$$\hat{g}^{n+1} = -\frac{i\epsilon v \cdot k}{1 + i\epsilon v \cdot k}\hat{\rho}^* \mathcal{F},$$

which integrates over the velocity v gives, in the limit of $\epsilon \to 0$,

$$\epsilon^{-\alpha} \left\langle \hat{g}^{n+1} \right\rangle = -\epsilon^{-\alpha} \int \frac{i\epsilon v \cdot k}{1 + i\epsilon v \cdot k} \mathcal{F}\,\mathrm{d}v \hat{\rho}^* \to -\kappa |k|^\alpha \hat{\rho}^*,$$

as shown in (2.15). Plug it into the Fourier transform of the first equation in (3.12), one obtains as $\epsilon \to 0$,

$$\frac{\hat{\rho}^{n+1} - \hat{\rho}^n}{\Delta t} = \epsilon^{-\alpha} \left\langle \hat{g}^{n+1} \right\rangle = -\kappa |k|^\alpha \hat{\rho}^*,$$

which gives a first order discretization of the limit equation (2.4).

When ρ^* is chosen as ρ^{n+1}, the scheme has the following properties.

Proposition 7. *The first order semi-discrete scheme (3.12) with $\rho^* = \rho^{n+1}$ conserves the total mass and dissipates the $L^2_{\mathcal{F}^{-1}}$ energy for all $\triangle t$.*

Proposition 8. *The first order semi-discrete scheme (3.12) with $\rho^* = \rho^{n+1}$ is unconditionally stable. More precisely, the energy E_ρ and E_g defined by (3.9) is uniformly bounded in time.*

Proposition 7 and 8 are discrete analogies of Proposition 5 and 6. The proofs are presented in Appendix A and B for completeness.

3.3 Velocity space truncation and Tail compensation

In the classical diffusion case where the equilibrium $\mathcal{F}$ takes the form of Gaussian distribution, one can truncate the velocity v within a certain domain when solving it numerically. However, if $\mathcal{F}$ has the form of (2.2), truncating it in any domain may introduce a huge error, especially for small ϵ where the information hidden in the tail becomes significant. Indeed, as written in (2.15), a truncation of v in $|v| < v_{\max}$ brings in an error

$$\frac{1}{\epsilon^\alpha} \int_{|v|>v_{\max}} \frac{(\epsilon v \cdot k)^2}{1 + (\epsilon v \cdot k)^2} \frac{\kappa_0}{|v|^{N+\alpha}} \, \mathrm{d}v \sim \frac{\kappa_0 S^{N-1}}{\alpha} \frac{1}{v_{\max}^\alpha} |k|^\alpha, \tag{3.13}$$

which implies that in order to suppress the error to $O(\epsilon)$, $v_{\max}$ should be chosen $O(\epsilon^{-\frac{1}{\alpha}})$, very expensive for small ϵ. Furthermore, this makes the scheme not AP since in an AP scheme the numerical parameters should be ϵ-independent. In fact, with any ϵ-independent finite truncation, the limit equation becomes the classical diffusion since the second order moment of the equilibrium $\mathcal{F}$ exists. We will show this in more detail with numerics in Section 5.1.

To overcome this difficulty, we further decompose $\mathcal{F}$ and g into

$$\mathcal{F}(v) = \mathcal{F}_{_B}(v) + \mathcal{F}_{_T}(v), \quad g(t,x,v) = g_{_B}(t,x,v) + g_{_T}(t,x,v), \tag{3.14}$$

where $\mathcal{F}_{_B}$ and $g_{_B}$ support on the domain of $|v| \le v_{\max}$ representing the 'body' part, while $\mathcal{F}_{_T}$ and $g_{_T}$ are zero when $|v| < v_{\max}$ incorporating the tail effect, i.e.,

$$\begin{aligned} \mathcal{F}_{_B}(v) &= \mathcal{F}(v)\mathbf{1}_{|v|\le v_{\max}}, \qquad \mathcal{F}_{_T}(v) = \mathcal{F}(v)\mathbf{1}_{|v|>v_{\max}}, \\ g_{_B}(v) &= g(v)\mathbf{1}_{|v|\le v_{\max}}, \qquad g_{_T}(v) = g(v)\mathbf{1}_{|v|>v_{\max}}. \end{aligned} \tag{3.15}$$

Equations (3.3) (3.4) then rewrite

$$\epsilon^\alpha \partial_t \rho = \left\langle g_{_B} + g_{_T} \right\rangle, \tag{3.16}$$

$$\epsilon^\alpha \partial_t g_{_B} + \epsilon v \cdot \nabla_x (\rho \mathcal{F}_{_B} + g_{_B}) = -g_{_B}, \tag{3.17}$$

$$\epsilon^\alpha \partial_t g_{_T} + \epsilon v \cdot \nabla_x (\rho \mathcal{F}_{_T} + g_{_T}) = -g_{_T}. \tag{3.18}$$

In a grid based numerical method one needs to truncate the velocity space at $|v| < v_{\max}$ and place finite number of grids in $[-v_{\max}, v_{\max}]$. Therefore $g_{_T}$ cannot be represented by values on grids. Here we propose the following ideas based on adding an *integrated tail* wisely.

- For a prescribed error δ, the truncation $v_{\max}$ is chosen according to

$$\int_{|v|>v_{\max}} \mathcal{F}\,\mathrm{d}v < \delta. \tag{3.19}$$

  Therefore, in a first order method, one can take $\delta = \mathcal{O}(\Delta t)$.

- $g_{_T}$ is approximated by its steady state. Then it solves

$$\epsilon v \cdot \nabla_x(\rho \mathcal{F}_{_T} + g_{_T}) = -g_{_T}.$$

  Now apply the Fourier Transform in x, the functions with a hat now depend on the frequency variable k. Hence the average $\langle \hat{g}_{_T} \rangle$ is given by

$$\frac{1}{\epsilon^\alpha}\langle \hat{g}_{_T} \rangle = \frac{1}{\epsilon^\alpha}\int_{|v|\geq v_{\max}} \frac{i\epsilon v\cdot k}{1+i\epsilon v\cdot k}\mathcal{F}(v)\,\mathrm{d}v\hat{\rho} = \frac{1}{\epsilon^\alpha}\int_{|v|\geq v_{\max}} \frac{(\epsilon v\cdot k)^2}{1+(\epsilon v\cdot k)^2}\frac{\kappa_0}{|v|^{N+\alpha}}\,\mathrm{d}v\hat{\rho} := C(k)\hat{\rho}, \tag{3.20}$$

  where $C(k)$ is precomputed numerically with any accuracy.

The assumption on $g_{_T}$ of being at steady state is based on the fact that $\epsilon^\alpha \partial_t g_{_T}$ is a higher order term for small ϵ, thus its form (3.20) is only valid when ϵ is small. This leads to a criteria of choosing $v_{\max}$. That is, $\frac{1}{\epsilon^\alpha}\langle g_{_T}\rangle$ should be of $\mathcal{O}(\triangle t)$ when $\epsilon \sim \mathcal{O}(1)$, which gives rises to (3.19). As a consequence, the truncation by $v_{\max}$ only introduces a first order error in $\triangle t$ if $\epsilon = \mathcal{O}(1)$. When $\epsilon \ll 1$, the evolution of $\langle g_{_T}\rangle$ in (3.20) gives a correct compensation to the limit equation (3.16). Then an AP property guarantees both the uniform stability and uniform accuracy of our scheme [11].

3.4 First order scheme

To this point, we are ready to write down the following first order scheme

$$\begin{cases} \epsilon^\alpha \dfrac{\rho^{n+1}-\rho^n}{\Delta t} = \left\langle g_{_B}^{n+1}\right\rangle + \left\langle g_{_T}^{n+1}\right\rangle, \\ \epsilon^\alpha \dfrac{g_{_B}^{n+1}-g_{_B}^n}{\Delta t} + \epsilon v\cdot\nabla_x(\rho^* \mathcal{F}_{_B} + g_{_B}^{n+1}) = -g_{_B}^{n+1}, \\ \dfrac{1}{\epsilon^\alpha}\left\langle \hat{g}_{_T}^{n+1}\right\rangle = -\dfrac{1}{\epsilon^\alpha}\displaystyle\int_{|v|\geq v_{\max}} \frac{i\epsilon v\cdot k}{1+i\epsilon v\cdot k}\mathcal{F}_{_T}(v)\,\mathrm{d}v\hat{\rho}^*, \end{cases} \tag{3.21}$$

where ρ^* can again be chosen as ρ^n or ρ^{n+1}. Then the distribution f is recovered at the last step from

$$f(t,x,v) = \rho(t,x)\mathcal{F}_{_B}(v) + g_{_B}(t,x,v), \qquad |v| \leq v_{\max}. \tag{3.22}$$

More specifically, we summarize the steps needed in our scheme. To begin with, denote

$$C(k) = \frac{1}{\epsilon^\alpha}\int_{|v|\geq v_{\max}} \frac{(\epsilon v\cdot k)^2}{1+(\epsilon v\cdot k)^2}\mathcal{F}_{_T}(v)\,\mathrm{d}v, \tag{3.23}$$

and precompute it with a prescribed accuracy (we can choose the velocity domain big enough to meet this accuracy). Here $v_{\max}$ is chosen according to (3.19). Then given $\left\langle \hat{g}_{_T}^n\right\rangle(k)$, $\hat{g}_{_B}^n(k,v)$ and $\hat{\rho}^n(k)$, we have, at time t^{n+1},

- Step 1. Compute $\frac{1}{\epsilon^\alpha}\left\langle \hat{g}_T^{n+1}(k,v)\right\rangle$ via

$$\frac{1}{\epsilon^\alpha}\left\langle \hat{g}_T^{n+1}(k,v)\right\rangle = -C(k)\hat{\rho}^*(k).$$

  If $\rho^* = \rho^n$, one can get the values for $\left\langle \hat{g}_T^{n+1}\right\rangle(k)$. If $\rho^* = \rho^{n+1}$, one writes $\left\langle \hat{g}_T^{n+1}\right\rangle(k)$ in terms of $\hat{\rho}^{n+1}(k)$.

- Step 2. Solve $\hat{g}_B^{n+1}(k,v)$ for $|v| \le v_{\max}$ from

$$\epsilon^\alpha \frac{\hat{g}_B^{n+1} - \hat{g}_B^n}{\Delta t} + i\epsilon v\cdot k(\hat{\rho}^*\mathcal{F} + \hat{g}_B^{n+1}) = -\hat{g}_B^{n+1}. \tag{3.24}$$

  Again if $\rho^* = \rho^n$, one can get the values for $\hat{g}_B^{n+1}$; and if $\rho^* = \rho^{n+1}$, one writes $\left\langle \hat{g}_B^{n+1}(k)\right\rangle$ in terms of $\hat{\rho}^{n+1}(k)$.

- Step 3. Compute $\left\langle \hat{g}_B^{n+1}\right\rangle$ by a simple summation of $\hat{g}_B^{n+1}$ in velocity space.

- Step 4. Plug $\frac{1}{\epsilon^\alpha}\left\langle \hat{g}_B^{n+1}\right\rangle$ and $\frac{1}{\epsilon^\alpha}\left\langle \hat{g}_T^{n+1}\right\rangle$ into

$$\hat{\rho}^{n+1} = \hat{\rho}^n + \frac{\triangle t}{\epsilon^\alpha}\left\langle \hat{g}_T^{n+1} + \hat{g}_B^{n+1}\right\rangle. \tag{3.25}$$

  to get $\hat{\rho}^{n+1}(k)$.

Repeat the above three steps until the end of time $t = t^M$, and f^M is recovered from

$$\hat{f}^M(k,v) = \rho^M(k)\mathcal{F}(v) + \hat{g}_B^M(k,v), \qquad \text{for } |v| \le v_{\max} \tag{3.26}$$

together with an inverse Fourier Transform.

The AP property can be checked formally. Taking the Fourier transform (in x direction) of the second equation in (3.21) and neglecting the high order term ϵ^α, one has

$$\hat{g}_B^{n+1} = -\frac{i\epsilon v\cdot k}{1 + i\epsilon v\cdot k}\hat{\rho}^*\mathcal{F}_B,$$

which together with the third equation in (3.21) lead to

$$\epsilon^{-\alpha}\left(\left\langle \hat{g}_B^{n+1}\right\rangle + \left\langle g_T^{n+1}\right\rangle\right) = -\epsilon^{-\alpha}\int \frac{i\epsilon v\cdot k}{1 + i\epsilon v\cdot k}(\mathcal{F}_B + \mathcal{F}_T)\,\mathrm{d}v\hat{\rho}^* \to -\kappa|k|^\alpha\hat{\rho}^*,$$

as shown in (2.15). Plug it into the Fourier transform of the first equation in (3.21), one obtains as $\epsilon \to 0$,

$$\frac{\hat{\rho}^{n+1} - \hat{\rho}^n}{\Delta t} = \epsilon^{-\alpha}\left\langle \hat{g}^{n+1}\right\rangle = -\kappa|k|^\alpha\hat{\rho}^*,$$

which again gives a first order discretization of the limit equation (2.4).

As mentioned in the last section, the choice of $v_{\max}$ in (3.19) guarantees the accuracy of our scheme when $\epsilon = \mathcal{O}(1)$, and the AP property here assure the accuracy when $\epsilon \ll 1$. Therefore, we have uniform accuracy in our scheme.

Remark 9. It is worth checking the total mass conservation. Denote $M^n = \int \rho^n + \left\langle g_{_B}^n \right\rangle + \left\langle g_{_T}^n \right\rangle \,\mathrm{d}x$, $n \geq 0$, the mass at time step t^n, then we have $M^n \equiv M^0$, which implies that the mass is conserved during the implementation of (3.21). Indeed, first from the third equation of (3.21), one sees that $\int \left\langle g_{_T}^n \right\rangle \,\mathrm{d}x \equiv 0$ for any $n \geq 1$. Then integrating the second equation w.r.t v, adding to the first one and then integrating over x, one immediately has

$$M^{n+1} = M^n + \frac{\Delta t}{\epsilon^\alpha} \int \left\langle g_{_T}^{n+1} \right\rangle \,\mathrm{d}x = M^n$$

for $n \geq 1$. On the other hand, from the initial decomposition (3.5), we have $\left\langle g_{_T}^0 \right\rangle = \int_{|v|>v_{\max}} (f_{\mathrm{in}} - \rho_{\mathrm{in}}\mathcal{F})\,\mathrm{d}v \sim \mathcal{O}(\Delta t)$ thanks to (3.19), which gives rise to $M^0 - \int f_{\mathrm{in}}\,\mathrm{d}x\,\mathrm{d}v \sim \mathcal{O}(\Delta t)$. Therefore, our scheme preserves the mass with an $\mathcal{O}(\Delta t)$ error. This error comes from the initial truncation, and it will not accumulate later on.

Remark 10. As an alternative, since $g_{_B}$ and $\langle g_{_B} \rangle$ have different orders, we can split $g_{_B}$ further into two parts $g_{_B} = \epsilon g + \epsilon^\alpha h$, and then decompose f into

$$f(t,x,v) = \rho(t,x)\mathcal{F}(v) + \epsilon g(t,x,v) + \epsilon^\alpha h(t,x,v) + g_{_T}(t,x,v).$$

Now we require $\langle g \rangle = 0$, whereas h and $\langle h \rangle$ have the same order of magnitude. Then the system splits

$$\begin{cases} \partial_t \rho = \langle h \rangle + \dfrac{1}{\epsilon^\alpha} \left\langle g_{_T} \right\rangle, \\ \epsilon^\alpha \partial_t g + v \cdot \nabla_x \rho_0 \mathcal{F} = -g, \\ \epsilon^\alpha \partial_t h + \epsilon^{2-\alpha} v \cdot \nabla_x g + \epsilon v \cdot \nabla_x h = -h, \\ \langle \hat{g}_{_T} \rangle = -\displaystyle\int_{|v| \geq v_{\max}} \frac{i\epsilon v \cdot k}{1 + i\epsilon v \cdot k} \mathcal{F}(v)\,\mathrm{d}v \hat{\rho}. \end{cases} \tag{3.27}$$

Here one sees that if $\langle g \rangle = 0$ initially and it remains so according to its evolution. In the limit of $\epsilon \to 0$, we have $\langle h \rangle \to 0$ and $\frac{1}{\epsilon^\alpha} \left\langle \hat{g}_{_T} \right\rangle \to -\kappa \left(-\triangle\right)^{\frac{\alpha}{2}} \rho$, which leads to the correct fractional diffusion.

3.5 A second order scheme

To get a second order AP scheme, we use the backward difference formula in time for the split system (3.3) (3.4) as follows

$$\begin{cases} \epsilon^\alpha \dfrac{3\rho^{n+1} - 4\rho^n + \rho^{n-1}}{2\Delta t} = \left\langle g_{_B}^{n+1} \right\rangle + \left\langle g_{_T}^{n+1} \right\rangle, \\ \epsilon^\alpha \dfrac{3g_{_B}^{n+1} - 4g_{_B}^n + g_{_B}^{n-1}}{2\Delta t} + \epsilon v \cdot \nabla_x (\rho^* \mathcal{F}_{_B} + g_{_B}^{n+1}) = -g_{_B}^{n+1}, \\ \left\langle \hat{g}_{_T}^{n+1} \right\rangle = -\displaystyle\int_{|v| \geq v_{\max}} \frac{i\epsilon v \cdot k}{1 + i\epsilon v \cdot k} \mathcal{F}_{_T}(v)\,\mathrm{d}v \hat{\rho}^*. \end{cases} \tag{3.28}$$

where $\rho^* = 2\rho^n - \rho^{n-1}$ for an explicit scheme and $\rho^* = \rho^{n+1}$ for an implicit scheme. Here we choose a cutoff $v_{\max}$ which makes $\delta = O(\Delta t^2)$ in (3.19). The AP property of this scheme simply follows that in the first order scheme, and in the limit $\epsilon \to 0$ it leads to

$$\frac{3\hat{\rho}^{n+1} - 4\hat{\rho}^n + \hat{\rho}^{n-1}}{2\Delta t} = -\kappa |k|^\alpha \hat{\rho}^*,$$

in the Fourier space. It is a second order discretization for the fractional diffusion equation.

4 Numerical scheme for space inhomogenous cross section

When the scattering cross section $\phi(x)$ only depends on x, the kinetic equation we will solve becomes

$$\epsilon^\alpha f_t + \epsilon v \cdot \nabla_x f = \nu(x) \left(\langle f \rangle \mathcal{F} - f \right), \tag{4.1}$$

where the collision frequency $\nu(x)$ is simply $\phi(x)$ in this case. In view of (4.1) and (3.1), the difference comes from an extra frequency function $\nu(x)$ in the collision, and the decomposition that builds on the Hilbert expansion still apply. But the Fourier Transform no longer fits for the spatial derivatives as it leads to a convolution which is hard to invert. In this section, we will first extend the major components of the scheme to the space inhomogenous cross section case, and then simplify the schemes in one dimension by a change of variable so that it is amenable to the Fourier Transform.

Decompose f again into a macro and a micro parts as in (3.2), then equation (4.1) is splited into

$$\begin{aligned} \epsilon^\alpha \partial_t \rho &= \nu(x) \langle g \rangle, & (4.2) \\ \epsilon^\alpha \partial_t g + \epsilon v \cdot \nabla_x (\rho \mathcal{F} + g) &= -\nu(x) g. & (4.3) \end{aligned}$$

Thus a first order semi-discrete scheme reads

$$\begin{cases} \epsilon^\alpha \dfrac{\rho^{n+1} - \rho^n}{\triangle t} = \nu(x) \left\langle g^{n+1} \right\rangle, \\ \epsilon^\alpha \dfrac{g^{n+1} - g^n}{\triangle t} + \epsilon v \cdot \nabla_x (\rho^* \mathcal{F} + g^{n+1}) = -\nu(x) g^{n+1}. \end{cases} \tag{4.4}$$

To check the AP property, denote $\Gamma(g) = \nu(x) g + \epsilon v \cdot \nabla_x g$, then the second equation in (4.4), upon neglecting the higher order terms, gives rise to

$$\Gamma(g^{n+1}) = -\epsilon v \cdot \nabla_x \rho^* \mathcal{F}, \tag{4.5}$$

in which one can solve for $g^{n+1}(x, v)$

$$g^{n+1}(x, v) = -\Gamma^{-1} \left(\epsilon v \cdot \nabla_x \rho^* \mathcal{F} \right) = -\int_0^\infty e^{-\int_0^z \nu(x - \epsilon v s) ds} \epsilon v \cdot \nabla_x \rho^* (x - \epsilon v z) \mathcal{F}(v) \, \mathrm{d}z. \tag{4.6}$$

Hence its average becomes

$$\frac{\nu(x)}{\epsilon^\alpha} \left\langle g^{n+1} \right\rangle = -\frac{\nu(x)}{\epsilon^\alpha} \int \mathrm{d}v \int_0^\infty e^{-\int_0^z \nu(x - \epsilon v s) ds} \epsilon v \cdot \nabla_x \rho^* (x - \epsilon v z) \mathcal{F}(v) \, \mathrm{d}z, \tag{4.7}$$

which in the limit of $\epsilon \to 0$ leads to $L(\rho^*)$ with L given in (2.18) (see [1] for more details).

As with the space homogeneous case, one needs to add an integrated tail when there is a truncation in the velocity space. Therefore, a scheme similar to (3.21) takes the following form

$$\begin{cases} \epsilon^\alpha \dfrac{\rho^{n+1} - \rho^n}{\Delta t} = \nu(x) \left\langle g_B^{n+1} \right\rangle + \nu(x) \left\langle g_T^{n+1} \right\rangle, \\ \epsilon^\alpha \dfrac{g_B^{n+1} - g_B^n}{\Delta t} + \epsilon v \cdot \nabla_x (\rho^* \mathcal{F}_B + g_B^{n+1}) = -\nu(x) g_B^{n+1}, \\ \dfrac{1}{\epsilon^\alpha} \left\langle g_T^{n+1} \right\rangle = -\dfrac{1}{\epsilon^\alpha} \displaystyle\int_{|v| \geq v_{\max}} \Gamma^{-1} \left(v \cdot \nabla_x \rho^* \mathcal{F}_T(v) \right) \mathrm{d}v, \end{cases} \tag{4.8}$$

where $g_{B/T}$ and $\mathcal{F}_{B/T}$ are defined in (3.15). Although the inverse operator Γ^{-1} takes a complicated form (4.6), numerically we can still single out the v dependence in the tail equation in (4.8) such that it can be precomputed. Let $(x_1, x_2, \cdots, x_N)$ be a discretization in x space, and denote

$$\mathbf{g}^n(v) = (g^n(x_1, v), g^n(x_2, v), \cdots, g^n(x_N, v)),$$

thus $\mathbf{g}^n$ is a $N \times 1$ vector for every v. Denote $\mathbf{\Gamma}(v)$ and $\mathbf{D}$ the matrix representations of the discretized operator Γ (for every v) and ∇_x, then we have from (4.5),

$$\mathbf{\Gamma}(v)\mathbf{g}^{n+1}(v) = -\epsilon v \mathbf{D}\rho^* \mathcal{F}(v).$$

where $\rho^* = (\rho^*(x_1), \rho^*(x_2), \cdots, \rho^*(x_N))$. Therefore, the integrated tail $\frac{1}{\epsilon^\alpha}\left\langle \mathbf{g}_{_T}^{n+1} \right\rangle$ takes the form of

$$\frac{1}{\epsilon^\alpha}\left\langle \mathbf{g}_{_T}^{n+1} \right\rangle = -\epsilon^{1-\alpha} \int_{|v|\geq v_{\max}} \mathbf{\Gamma}(v)^{-1}\mathbf{D} v \mathcal{F}(v)\, \mathrm{d}v \rho^* := \mathbf{C}\rho^*, \tag{4.9}$$

where the matrix $\mathbf{C}$ can be precomputed.

Since matrix $\mathbf{C}$ has dimension $N \times N$, precomputing it may still need a substantial effort. Here we offer an alternative approach for one dimension (i.e., $x \in R$) which significantly simplifies this computation. Consider a change of variable such that in the tail equation

$$\epsilon v \partial_x \left(\rho \mathcal{F}_{_T} + g_{_T}\right) = -\nu(x) g_{_T}, \tag{4.10}$$

the $x-$dependent function $\nu(x)$ can be grouped onto the left hand side. More precisely, let $y = y(x)$ such that $y'(x) = \nu(x)$. Then (4.10), upon change of variable from x to y, becomes

$$\epsilon v \partial_y (\rho \mathcal{F}_{_T} + g_{_T}) = -g_{_T}, \tag{4.11}$$

where $g_{_T}$ can be readily solved by the Fourier Transform. Then apply the same transform to (4.8), it becomes

$$\begin{cases} \epsilon^\alpha \dfrac{\tilde{\rho}^{n+1} - \tilde{\rho}^n}{\Delta t} = \tilde{\nu}(y)\left\langle \tilde{g}_{_B}^{n+1} \right\rangle + \tilde{\nu}(y)\left\langle \tilde{g}_{_T}^{n+1} \right\rangle, \\ \dfrac{\epsilon^\alpha}{\hat{\nu}(y)} \dfrac{\tilde{g}_{_B}^{n+1} - \tilde{g}_{_B}^n}{\Delta t} + \epsilon v \cdot \nabla_y (\tilde{\rho}^* \mathcal{F}_{_B} + \tilde{g}_{_B}^{n+1}) = -\tilde{g}_{_B}^{n+1}, \\ \left\langle \hat{\tilde{g}}_{_T}^{n+1} \right\rangle = \displaystyle\int_{|v|\geq v_{\max}} \frac{i\epsilon v \cdot k}{1 + i\epsilon v \cdot k} \mathcal{F}(v)\, \mathrm{d}v \hat{\tilde{\rho}}, \end{cases} \tag{4.12}$$

where $\tilde{\rho}(t, y, v) = \rho(t, x, v)$, $\tilde{\nu}(t, y, v) = \nu(t, x, v)$, and their Fourier transform with respect to y are denoted by $\hat{\tilde{g}}(t, k, v)$ and $\hat{\tilde{\rho}}(t, k, v)$.

Remark 11. Note that the limit of (4.12) as $\epsilon \to 0$ solves the equation

$$\partial_t \tilde{\rho} = -\kappa(-\triangle_y)^{\frac{\alpha}{2}} \tilde{\rho}\tilde{\nu}(y) \tag{4.13}$$

with κ given by (2.5). On the other hand, the limit of (4.8) as $\epsilon \to 0$ solves the system (2.17)-(2.19). This actually provides us an alternative way to solve the one dimensional limit system (2.17)(2.18), if the function $\gamma(x, y)$ in (2.18) is defined through a function $\nu(x)$ as in (2.19). More specifically, to solve (2.17)-(2.19), one can

1. Introduce a variable $y = y(x)$ such that $y'(x) = \nu(x)$. Let $\tilde{\rho}(y) := \rho(x(y))$.
2. Solve the system (4.13). If a periodic boundary condition in x is assumed, one can simply use FFT to solve $(-\triangle_y)^{\frac{\alpha}{2}} \tilde{\rho}$.
3. At the time t, the function $\rho(x) = \tilde{\rho}(y)$ gives the solution of the system (2.17)-(2.19) at the points $x = x(y)$.

This is checked numerically in Section 5.6.

5 Numerical Examples

In this section, we perform several numerical tests using our numerical schemes (3.21), (3.28), and (4.12) in both kinetic and fractional diffusive regimes. Here the spatial domain is chosen $x \in [0, 2\pi]$ with periodic boundary condition, and its discretization is treated via a spectral method (the Fourier Transform). The velocity space is chosen according to (3.19), and the integration in the tail is obtained through a simple mid-point rule.

5.1 Tail Effect

The first test is devoted to demonstrate the effect of $v_{\max}$, and address the need of adding the tail. We compute the following integral in the truncated one dimensional velocity space $\{|v| < v_{\max}\}$,

$$I_1(k) := \lim_{\epsilon \to 0} \frac{1}{\epsilon^\alpha} \int_{|v|<v_{\max}} \frac{i\epsilon v \cdot k}{1 + i\epsilon v \cdot k} \mathcal{F}(v)\, \mathrm{d}v, \tag{5.1}$$

which constitutes the source term g_B in the limit of equation (3.16). Figure 1 displays the integral $I_1(k)$ with different cutoff $v_{\max}$. Here we take $\alpha = 1.5$. It shows that high frequency satisfies $I_1(k) = O(|k|^\alpha)$, whereas low and moderate frequencies (for example $|k| < 10^3$ with $v_{\max} = 10^5$) lead to $I_1(k) = O(|k|^2)$. Therefore, the limit as $\epsilon \to 0$ in truncated velocity space behaves like classical diffusion, instead of a fractional diffusion that is derived by integrating over the whole domain (Lemma 2).

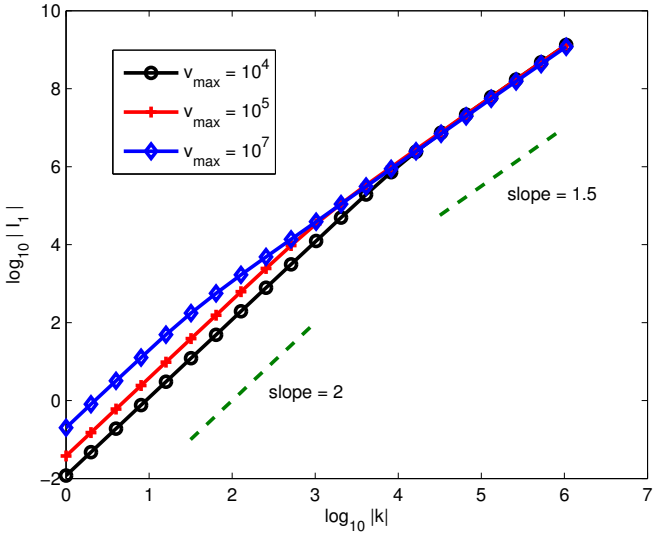

Figure 1: The integral I_1 in (5.1) as a function of the frequency k, with different cutoff $v_{\max}$ in velocity space.

5.2 Test on the asymptotic orders

To obtain the asymptotic preserving property of the first order scheme (3.12), we have neglected the term $\epsilon^\alpha \frac{g^{n+1}-g^n}{\Delta t}$ in the second equation as it is a high order term as $\epsilon \to 0$. In this test we check its magnitude numerically.

We solve the problem with $\alpha = 1.5$ on $x \in [0, 2\pi]$, starting with the *non-equilibrium* initial value

$$\rho(x) = e^{-5(x-\pi)^2}, \quad f(x) = \frac{\rho(x)}{\sqrt{2\pi}} e^{-|v|^2/2}. \tag{5.2}$$

We take $N_x = 100$, which gives satisfactory accuracy in Δx since we apply a spectral method in x direction. Denote

$$R_\epsilon(t^n) = \frac{||\epsilon^\alpha (g^{n+1} - g^n)/\Delta t||}{||g^n||}, \tag{5.3}$$

with $||\cdot||$ defined by the energy norm

$$||\psi|| = \left(\iint \psi^2 \mathcal{F}^{-1} \, \mathrm{d}x \, \mathrm{d}v \right)^{1/2}.$$

As shown in Figure 2, this ratio scales like ϵ^α as $\epsilon \to 0$. This confirms that the time derivative $\epsilon^\alpha \frac{g^{n+1}-g^n}{\Delta t}$ is a high order term compared to the right hand side of the second equation of (3.12). It can be neglected when we study the AP property.

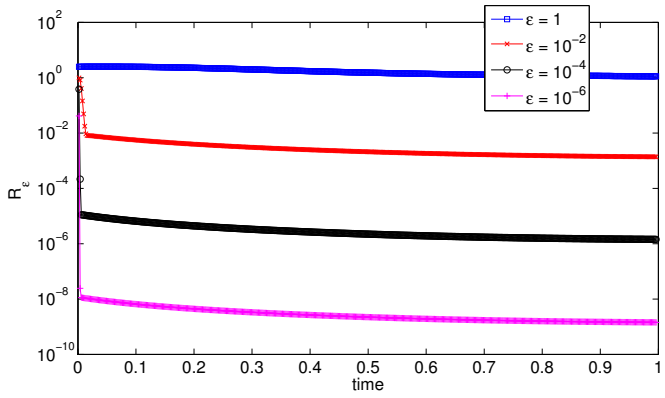

Figure 2: The evolution of the ratio R_ϵ in (5.3) for different α.

5.3 Convergence test

In this section we perform the convergence test on the first order scheme (3.21) and the second order scheme (3.28), in both the explicit and the implicit settings. The same initial condition in (5.2) is used. The simulation is performed up to time $T = 0.5$, with the numbers of time steps $N_t = 200, 400, 800, 1600$ and 3200. We take the cutoff $v_{\max} = 40$, which is large enough to satisfy (3.19) with $\delta = O(\Delta t^2)$. In Figure 3 the explicit first order and second order methods are tested and the expected convergence orders are observed. Figure 4 gives similar results with the implicit methods.

5.4 Stability test

We now check the dissipation of energy (3.6) for the combined solution $\rho\mathcal{F} + g$, and the boundedness of energy (3.9) for each component ρ and g. The initial value (5.2) is used, with $\alpha = 1.5$ and the cutoff $v_{\max} = 100$. The first order implicit schemes, (3.21) with $\rho^* = \rho^{n+1}$, is applied. In the left of Figure 5, the kinetic regime with $\epsilon = 1$ is studied. E_f decays as shown in Proposition 7. E_ρ and

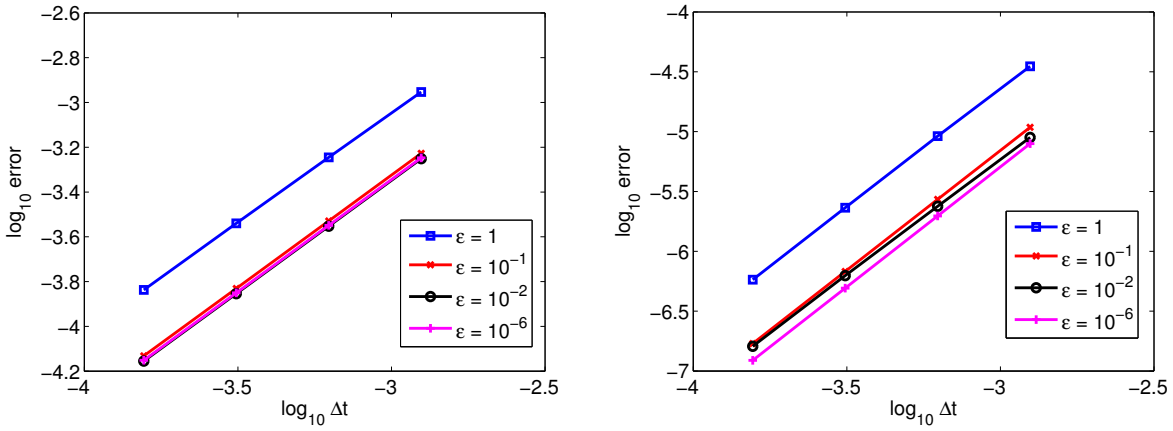

Figure 3: Convergence test for the first order (left) and second order (right) explicit AP schemes for different ϵ. Here we take $\alpha = 1.5$, $v_{\max} = 40$.

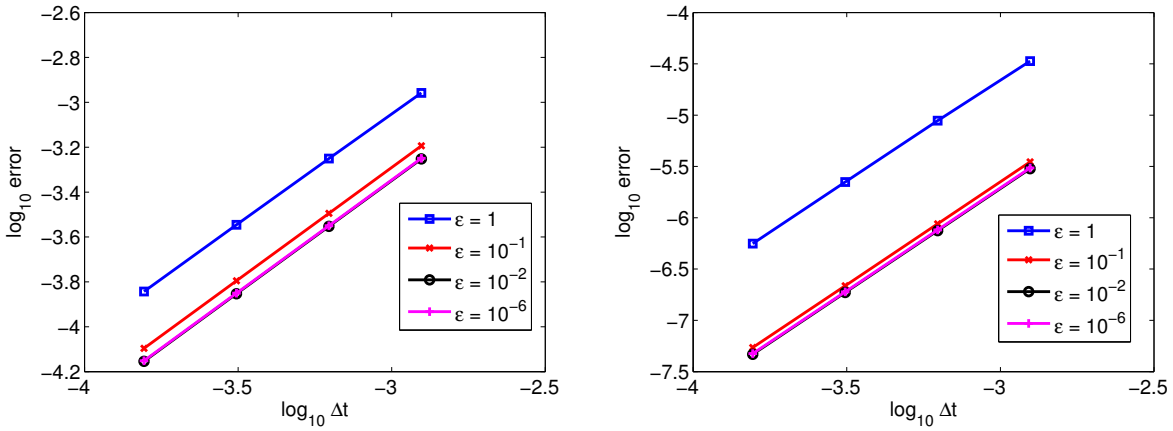

Figure 4: Convergence test for the first order (left) and second order (right) implicit AP schemes. $\alpha = 1.5$ for different ϵ. Here we take $\alpha = 1.5$, $v_{\max} = 40$.

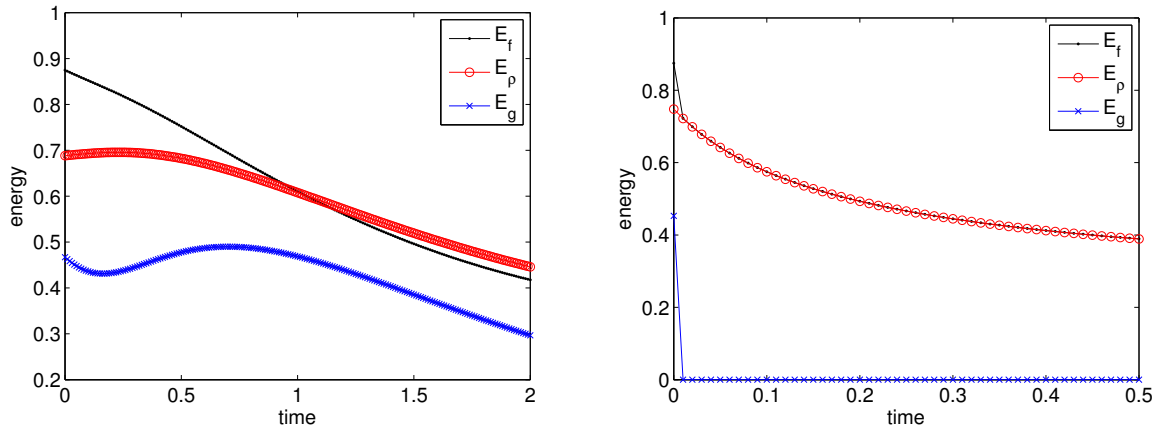

Figure 5: Decay of energy E_f defined in (3.6), and the boundedness of E_ρ and E_g defined in (3.9), for the first order implicit AP scheme. Here $\epsilon = 1$ in the left, $\epsilon = 10^{-6}$ in the right. We take $\alpha = 1.5$ and $v_{\max} = 100$.

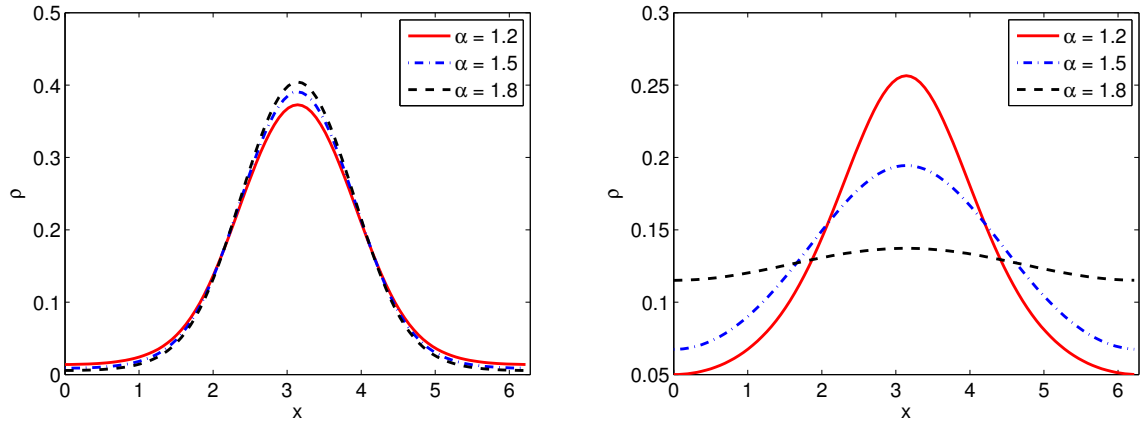

Figure 6: The density function ρ at time $T = 1$, with $\epsilon = 1$ (left) and $\epsilon = 10^{-6}$, for different α.

E_g, though not monotonically decreasing, are bounded over time. This shows the stability of our scheme. The same results are observed in the diffusive regime with $\epsilon = 10^{-6}$, as shown in the right of Figure 5. Furthermore, the sudden change in E_f and E_g at the first time step is due to the fact that the initial value (5.2) is not at equilibrium.

At last, we would like to point out that, in spite of the lack of theoretical support, the explicit methods also exhibits the similar properties.

5.5 Different α

In this section we study the effect due to different α. Again the initial value (5.2) is used, with the cutoff $v_{\max} = 100$. In Figure 6 we report the density function ρ at time $T = 1$, with $\epsilon = 1$ (left) and $\epsilon = 10^{-6}$, for $\alpha = 1.2$, 1.5 and 1.8. In the right figure where $\epsilon = 10^{-6}$, the solution with a larger α clearly exhibits a stronger diffusion. This coincides with the corresponding asymptotic limits. For a smaller ϵ, this coincidence is missing. In fact, as shown in the left of Figure 6, the solution with a larger α leads to a smaller "diffusion".

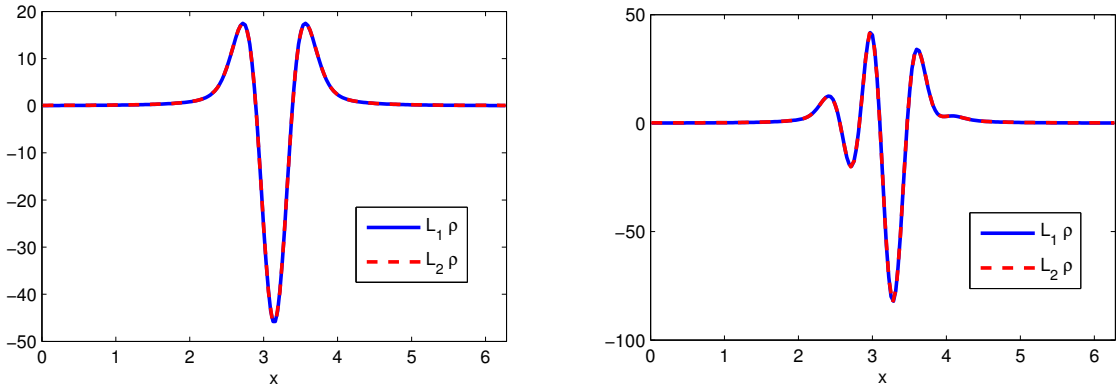

Figure 7: The functions $L_1\rho_k$ (solid line) and $L_2\rho_k$ (dash line) defined in (5.4), for the two density ρ_1 (left) and ρ_2 (right) defined in (5.5). $N_x = 200$ points are used. $\alpha = 1.5$.

5.6 Spatial Inhomogeneous Kernel

5.6.1 Numerical verification of Remark 11

Now we study the kinetic system (4.1) where the cross section $\nu(x)$ is spatially inhomogeneous. First we numerically check Remark 11. More specifically, we check the following two operator are equivalent in one dimension

$$\begin{aligned} L_1\rho(x) &= \kappa_0 P.V. \int_{\mathbf{R}} \gamma(x,z)\frac{\rho(x)-\rho(z)}{|x-z|^{\alpha+1}}\,\mathrm{d}z, \\ L_2\rho(x) &= \tilde{L_2}\tilde{\rho}(y(x)) = -\kappa(-\triangle_y)^{\frac{\alpha}{2}}\tilde{\rho}\tilde{\nu}(y), \end{aligned} \tag{5.4}$$

where $\frac{\mathrm{d}y(x)}{\mathrm{d}x} = \nu(x)$, κ is given by (2.5), and γ is defined through ν by (2.19).

We take $\nu(x) = 1 + 0.4\cos(x)$ and apply L_1 and L_2 to two different density functions

$$\begin{aligned} \rho_1(x) &= e^{-10(x-\pi)^2}, \\ \rho_2(x) &= (1 + 0.5\sin(8x))e^{-5(x-\pi)^2}. \end{aligned} \tag{5.5}$$

$L_1\rho_k$ and $L_2\rho_k$ are shown in Figure. They agree very well with each other.

5.6.2 AP property

Next we show that the AP property of the scheme (4.12). We only need to show its limit as $\epsilon \to 0$ solves (4.13), since (4.13) and the system (2.17)-(2.19) are equivalent. We start with the equilibrium initial distribution $f = \rho\mathcal{F}$, with ρ given by ρ_2 in (5.5). In Figure 8 we compare the solution obtained from (4.12) with $\epsilon = 10^{-8}$ (blue solid line) and that by solving (4.13), at various time. The good agreement suggest that the scheme (4.12) is asymptotic preserving.

6 Conclusion

We designed an asymptotic preserving scheme for linear Boltzmann equation with fractional diffusion limit. When the local equilibrium is not a Maxwellian but rather a heavy tail function with power law decay, the classical diffusion theory fails because the second moment of the equilibrium

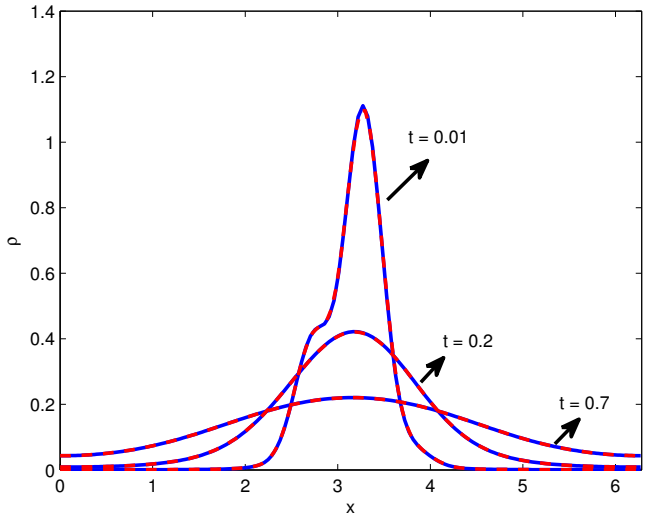

Figure 8: The snapshots of the density ρ obtained from (4.12) with $\epsilon = 10^{-8}$ (blue solid line) and that by solving (4.13) (red dashed line), at various time. $N_x = 200$ points are used. $\alpha = 1.5$.

is infinite which renders the diffusion matrix unbounded. Instead, we consider a new time scale that gives rise to the fractional diffusion limit, but also leads to a severe difficulty in numerical realization as the Hilbert expansion in the classical diffusion no longer applies. To overcome this difficulty, we propose a novel micro-macro decomposition for the distribution function, which splits the original kinetic equation following a *reshuffled* Hilbert expansion. Such a splitting is proved to be stable. Another major difficulty comes from the fat tail that disables any truncation in the velocity space numerically. Our idea is to incorporate an *integrated tail* whose major component can be precomputed with any accuracy. We analyzed the asymptotic behavior of the numerical scheme, and prove its unconditionally stability for a fully implicit scheme. Several numerical results are carried out to confirm the needs of adding the tail, as well as the properties of the scheme including asymptotic-preservation, uniform accuracy and energy dissipation.

References

[1] N. B. Abdallah, A. Mellet, and M. Puel, *Fractional diffusion limit for collisional kinetic equations: a hilbert expansion approach*, Kinetic Related Models, (2014).

[2] C. Bardos, R. Santos, and R. Sentis, *Diffusion approximation and computation of the critical size*, Trans. A. M. S., 284 (1984), pp. 617–649.

[3] A. Bensoussan, J. L. Lions, and G. Papanicolaou, *Boundary layers and homogenization of transport processes*, Publ. Res. Inst. Math. Sci., 15 (1979), pp. 53–157.

[4] A. V. Bobylev, J. A. Carrillo, and I. M. Gamba, *On some properties of kinetic and hydrodynamic equations for inelastic interactions*, J. Stat. Phys., 98 (2000), pp. 743–773.

[5] A. V. Bobylev and I. M. Gamba, *Boltzmann equations for mixtures of Maxwell gases: exact solutions and power like tails*, J. Stat. Phys., 124 (2006), pp. 497–516.

[6] N. Crouseilles, P. Degond, and M. Lemou, *A hybrid kinetic/fluid model for solving the gas dynamics boltzmann-bgk equation*, J. Comput. Phys., 199 (2004), pp. 776–808.

[7] ——, *A hybrid kinetic-fluid model for solving the vlasov-bgk equation*, J. Comput. Phys., 199 (2005), pp. 572–601.

[8] N. Crouseilles, H.Hivert, and M. Lemou, *Numerical schemes for kinetic equations in the diffusion and anomalous diffusion limits. parti: The case of heavy-tailed equilibrium*, preprint.

[9] P. Degond, T. Goudon, and F. Poupaud, *Diffusion limit for non homogeneous and non-micro-reversibles processes*, Indiana Univ. Math. J., 49 (2000), pp. 1175–1198.

[10] D. Duering and G. Toscani, *Anomalous diffusion limit induced on a kinetic equation*, Physica A, 384 (2007), pp. 493–506.

[11] F. Golse, S. Jin, and C. D. Levermore, *The convergence of numerical transfer schemes in diffusive regimes i: Discrete-ordinate method*, SIAM Journal on Numerical Analysis, 36 (1999), pp. pp. 1333–1369.

[12] S. Jin, *Asymptotic preserving (AP) schemes for multiscale kinetic and hyperbolic equations: a review*, Riv. Mat. Univ. Parma, 3 (2012), pp. 177–216.

[13] S. Jin, L. Pareschi, and G. Toscani, *Uniformly accurate diffusive relaxation schemes for multiscale transport equations*, SIAM J. Numer. Anal., 38 (2000), pp. 913–936.

[14] E. W. Larsen and J. B. Keller, *Asymptotic solution of neutron transport problems for small mean free path*, J. Math. Phys., 15 (1974), pp. 75–81.

[15] M. Lemou and L. Mieussens, *New asymptotic preserving scheme based on micro-macro formulation for linear kinetic equations in the diffusion limit*, SIAM J. Sci. Comput., 31 (2008), pp. 334–368.

[16] A. Mellet, *Fractional diffusion limit for collisional kinetic equations: A moments method*, Indiana Univ. Math. J., 59 (2010), pp. 1333–1360.

[17] A. Mellet, S. Mischler, and C. Mouhot, *Fractional diffusion limit for collisional kinetic equations*, Arch. Ration. Mech. Anal., 199 (2011), pp. 493–525.

[18] D. Summers and R. M. Thorne, *The modified plasma dispersion function*, Phys. Fluids., 83 (1991), pp. 1835–1847.

A Proof of Proposition 7

Proof. By integrating the first equation in (3.12) in x and second in both x and v, and adding them, one immediately gets $\int \rho^{n+1} + \langle g^{n+1} \rangle \, \mathrm{d}x = \int \rho^n + \langle g^n \rangle \, \mathrm{d}x$, which implies mass conservation. To show the stability, multiply the first equation in (3.12) by ρ^{n+1} and second by $g^{n+1}/\mathcal{F}$, one sees

$$\frac{\epsilon^\alpha}{2\Delta t}\left[(\rho^{n+1})^2 - (\rho^n)^2 + (\rho^{n+1}-\rho^n)^2\right] = \rho^{n+1}\left\langle g^{n+1}\right\rangle, \tag{A.1}$$

$$\frac{\epsilon^\alpha}{2\Delta t}\left[\frac{(g^{n+1})^2}{\mathcal{F}} - \frac{(g^n)^2}{\mathcal{F}} + \frac{\left(g^{n+1}-g^n\right)^2}{\mathcal{F}}\right] + \epsilon v\cdot\nabla_x(\rho^{n+1}\mathcal{F}+g^{n+1})\frac{g^{n+1}}{\mathcal{F}} = -\frac{(g^{n+1})^2}{\mathcal{F}}, \tag{A.2}$$

where we have used the equality $a(a-b) = a^2 - b^2 + (a-b)^2$. Integrating (A.1) in x and (A.2) in both x and v, and adding them together yield

$$\frac{\epsilon^\alpha}{2\triangle t}\iint\left[\frac{\left(\rho^{n+1}\mathcal{F}+g^{n+1}\right)^2}{\mathcal{F}}-\frac{\left(\rho^n\mathcal{F}+g^n\right)^2}{\mathcal{F}}\right]\mathrm{d}x\,\mathrm{d}v+\frac{\epsilon^\alpha}{2\triangle t}\iint\left[\left(\rho^{n+1}-\rho^n\right)^2\mathcal{F}+\frac{\left(g^{n+1}-g^n\right)^2}{\mathcal{F}}\right]\mathrm{d}x\,\mathrm{d}v$$
$$+\epsilon\int\left[\left\langle vg^{n+1}\cdot\nabla_x\rho^{n+1}\right\rangle+\left\langle v\cdot\nabla_x\frac{(g^{n+1})^2}{2\mathcal{F}}\right\rangle\right]\mathrm{d}x+\frac{\epsilon^\alpha}{\triangle t}\int\left(\rho^n\left\langle g^n\right\rangle-\rho^{n+1}\left\langle g^{n+1}\right\rangle\right)\mathrm{d}x$$
$$=\int\left[-\left\langle\frac{(g^{n+1})^2}{\mathcal{F}}\right\rangle+\rho^{n+1}\left\langle g^{n+1}\right\rangle\right]\mathrm{d}x. \tag{A.3}$$

Note that $\int\left\langle v\cdot\nabla_x\frac{(g^{n+1})^2}{2\mathcal{F}}\right\rangle\mathrm{d}x=0$ and

$$\frac{\epsilon^\alpha}{\triangle t}\int\left(\rho^n\left\langle g^n\right\rangle-\rho^{n+1}\left\langle g^{n+1}\right\rangle\right)\mathrm{d}x=\frac{\epsilon^\alpha}{\triangle t}\int\left[\left(\rho^n-\rho^{n+1}\right)\left\langle g^{n+1}\right\rangle+\rho^n\left\langle g^n-g^{n+1}\right\rangle\right]\mathrm{d}x$$
$$=-\int\left\langle g^{n+1}\right\rangle^2\mathrm{d}x+\int\rho^n\left\langle g^{n+1}\right\rangle\mathrm{d}x+\epsilon\int\rho^n\left\langle v\cdot\nabla_x g^{n+1}\right\rangle\mathrm{d}x, \tag{A.4}$$

then (A.3) rewrites

$$\frac{\epsilon^\alpha}{2\triangle t}\iint\left[\frac{\left(\rho^{n+1}\mathcal{F}+g^{n+1}\right)^2}{\mathcal{F}}-\frac{\left(\rho^n\mathcal{F}+g^n\right)^2}{\mathcal{F}}\right]\mathrm{d}x\,\mathrm{d}v$$
$$=\int\left[\left\langle(g^{n+1})^2\right\rangle-\left\langle\frac{(g^{n+1})^2}{\mathcal{F}}\right\rangle+\left(\rho^{n+1}-\rho^n\right)\left\langle g^{n+1}\right\rangle-\epsilon\left\langle vg^{n+1}\right\rangle\cdot\nabla_x\left(\rho^{n+1}-\rho^n\right)\right]\mathrm{d}x$$
$$-\frac{\epsilon^\alpha}{2\triangle t}\iint\left[\left(\rho^{n+1}-\rho^n\right)^2+\frac{\left(g^{n+1}-g^n\right)^2}{\mathcal{F}}\right]\mathrm{d}x\,\mathrm{d}v$$
$$=\int\left[\left\langle(g^{n+1})^2\right\rangle-\left\langle\frac{(g^{n+1})^2}{\mathcal{F}}\right\rangle\right]\mathrm{d}x-\frac{\epsilon^\alpha}{2\triangle t}\iint\left[\left(\rho^{n+1}-\rho^n\right)^2\mathcal{F}+\frac{\left(g^{n+1}-g^n\right)^2}{\mathcal{F}}\right]\mathrm{d}x\,\mathrm{d}v$$
$$+\int\left(\rho^{n+1}-\rho^n\right)\left\langle g^{n+1}+\epsilon v\nabla_x g^{n+1}\right\rangle\mathrm{d}x.$$

Notice that $\left\langle g^{n+1}+\epsilon v\nabla_x g^{n+1}\right\rangle=-\frac{\epsilon^\alpha}{\triangle t}\left\langle g^{n+1}-g^n\right\rangle$, we have

$$\int\left(\rho^{n+1}-\rho^n\right)\left\langle g^{n+1}+\epsilon v\nabla_x g^{n+1}\right\rangle\mathrm{d}x=-\frac{\epsilon^\alpha}{\triangle t}\int\left(\rho^{n+1}-\rho^n\right)\left\langle g^{n+1}-g^n\right\rangle\mathrm{d}x$$
$$\leq\frac{\epsilon^\alpha}{2\triangle t}\iint\left[\left(\rho^{n+1}-\rho^n\right)^2\mathcal{F}+\frac{\left(g^{n+1}-g^n\right)^2}{\mathcal{F}}\right]\mathrm{d}x\,\mathrm{d}v.$$

Similar to (3.7), we have $\int\left[\left\langle(g^{n+1})^2\right\rangle-\left\langle\frac{(g^{n+1})^2}{\mathcal{F}}\right\rangle\right]\mathrm{d}x\leq 0$. Therefore,

$$\frac{\epsilon^\alpha}{2\triangle t}\iint\left[\frac{\left(\rho^{n+1}\mathcal{F}+g^{n+1}\right)^2}{\mathcal{F}}-\frac{\left(\rho^n\mathcal{F}+g^n\right)^2}{\mathcal{F}}\right]\mathrm{d}x\,\mathrm{d}v\leq 0,$$

which ends the proof. □

B Proof of Proposition 8

Proof. By multiplying ρ^{n+1} to the both sides of the first equation in (3.12) and integrating over x, one has

$$\begin{aligned}
&\epsilon^\alpha \frac{(E_\rho^{n+1})^2 - (E_\rho^n)^2}{2\Delta t} + \frac{\epsilon^\alpha}{2\Delta t} \int (\rho^{n+1} - \rho^n)^2 \,\mathrm{d}x \\
=& \int \rho^{n+1} \left\langle g^{n+1} \right\rangle \,\mathrm{d}x \\
=& \iint \rho^{n+1} (\rho^{n+1} \mathcal{F} + g^{n+1}) \,\mathrm{d}v \,\mathrm{d}x - \int (\rho^{n+1})^2 \,\mathrm{d}x \\
\leq& \frac{1}{2} \iint \left((\rho^{n+1})^2 \mathcal{F} + (\rho^{n+1} \mathcal{F} + g^{n+1})^2 \mathcal{F}^{-1} \right) \,\mathrm{d}v \,\mathrm{d}x - \int (\rho^{n+1})^2 \,\mathrm{d}x \\
=& \frac{1}{2} ((E_\rho^{n+1})^2 + (E_f^{n+1})^2) - (E_\rho^{n+1})^2 \\
=& \frac{1}{2} ((E_f^{n+1})^2 - (E_\rho^{n+1})^2).
\end{aligned}$$

Therefore

$$\epsilon^\alpha \frac{(E_\rho^{n+1})^2 - (E_\rho^n)^2}{\Delta t} \leq (E_f^{n+1})^2 - (E_\rho^{n+1})^2.$$

Since E_f^n decays, one can easily see that E_ρ^n is uniformly bounded. Then from (3.11), E_g^n is also uniformly bounded.

□